Suppression of Ca²⁺ syntillas increases spontaneous exocytosis in mouse adrenal chromaffin cells

Jason J. Lefkowitz,[1,2] Kevin E. Fogarty,[2,3] Lawrence M. Lifshitz,[2,3] Karl D. Bellve,[2,3] Richard A. Tuft,[2,3] Ronghua ZhuGe,[2] John V. Walsh Jr.,[2] and Valerie De Crescenzo[2]

[1]Program in Neuroscience, [2]Department of Physiology, Biomedical Imaging Group, and [3]Program in Molecular Medicine, University of Massachusetts Medical School, Worcester, MA 01655

A central concept in the physiology of neurosecretion is that a rise in cytosolic [Ca²⁺] in the vicinity of plasmalemmal Ca²⁺ channels due to Ca²⁺ influx elicits exocytosis. Here, we examine the effect on spontaneous exocytosis of a rise in focal cytosolic [Ca²⁺] in the vicinity of ryanodine receptors (RYRs) due to release from internal stores in the form of Ca²⁺ syntillas. Ca²⁺ syntillas are focal cytosolic transients mediated by RYRs, which we first found in hypothalamic magnocellular neuronal terminals. (*scintilla*, Latin for spark; found in nerve terminals, normally synaptic structures.) We have also observed Ca²⁺ syntillas in mouse adrenal chromaffin cells. Here, we examine the effect of Ca²⁺ syntillas on exocytosis in chromaffin cells. In such a study on elicited exocytosis, there are two sources of Ca²⁺: one due to influx from the cell exterior through voltage-gated Ca²⁺ channels, and that due to release from intracellular stores. To eliminate complications arising from Ca²⁺ influx, we have examined spontaneous exocytosis where influx is not activated. We report here that decreasing syntillas leads to an increase in spontaneous exocytosis measured amperometrically. Two independent lines of experimentation each lead to this conclusion. In one case, release from stores was blocked by ryanodine; in another, stores were partially emptied using thapsigargin plus caffeine, after which syntillas were decreased. We conclude that Ca²⁺ syntillas act to inhibit spontaneous exocytosis, and we propose a simple model to account quantitatively for this action of syntillas.

INTRODUCTION

Since the work of Katz, Douglas, and their collaborators almost half a century ago (Katz, 1969), a central concept in the physiology of neurosecretion is that a rise in cytosolic [Ca²⁺], resulting from Ca²⁺ influx, triggers exocytosis. More recently it has become clear that the rise in [Ca²⁺] occurs in a microdomain within the vicinity (i.e., at a distance of 200–300 nm in chromaffin cells) of plasmalemmal Ca²⁺ channels (García et al., 2006; Neher and Sakaba, 2008). This finding raises the possibility of other microdomains where a rise in focal [Ca²⁺] might mediate other processes, allowing Ca²⁺ to subserve several functions without cross talk. This possibility receives further support from the study of Ca²⁺ sparks in smooth muscle cells. Ca²⁺ sparks are focal Ca²⁺ transients found in striated and smooth muscle and mediated by RYRs (Cheng and Lederer, 2008). In striated muscle, they are the quanta or building blocks that make up a global increase in [Ca²⁺] to trigger contraction (Csernoch, 2007). However, in smooth muscle, Ca²⁺ sparks have quite a different function. They activate large conductance Ca²⁺-activated K⁺ channels (BK channels) located within 150–300 nm of the spark site (ZhuGe et al., 2002); the resulting K⁺ efflux and hyperpolarization deactivates

voltage-gated Ca²⁺ channels and thus terminates contraction. Hence, in smooth muscle, sparks have quite the opposite function from that in striated muscle and the opposite of a global [Ca²⁺] in smooth muscle. In smooth muscle, sparks cause a relaxation (Nelson et al., 1995; ZhuGe et al., 1998).

Ca²⁺ syntillas are brief (on the order of tens of milliseconds), focal cytosolic Ca²⁺ transients due to release from intracellular stores and mediated by RYRs (De Crescenzo et al., 2004; Collin et al., 2005). They were first found in freshly isolated neurohypophysial terminals of magnocellular neurons (De Crescenzo et al., 2004). Because the transients resembled Ca²⁺ sparks found in muscle, we designated them Ca²⁺ syntillas (*scintilla*, Latin for spark; from a nerve terminal, normally a synaptic structure). In a previous study (ZhuGe et al., 2006), we also found such focal transients in freshly isolated mouse adrenal chromaffin cells, which resemble in their magnitude, time course and spontaneous frequency those found in neurohypophysial nerve terminals. That study established two main points: (1) syntillas in chromaffin cells arise from intracellular stores, as indicated by their occurrence in the absence of extracellular Ca²⁺; and (2) syntillas do not trigger exocytotic events, despite

their releasing sufficient Ca^{2+} to do so if the release were to occur within several hundred nanometers of a docked, primed dense core vesicle (DCV). Hence, we proposed that Ca^{2+} syntillas arise in a different microdomain from that of the docked, primed vesicle. However, we did not uncover the function of Ca^{2+} syntillas, the topic addressed here.

Here, we examine the effects of Ca^{2+} syntillas on exocytosis in mouse adrenal chromaffin cells. We have begun by studying spontaneous exocytosis in the form of individual exocytotic events as measured amperometrically. (We use the term "spontaneous" rather than "basal" exocytosis because a low level of stimulation is sometimes designated "basal" stimulation; e.g., Fulop et al., 2005.) There are three reasons for studying spontaneous exocytosis. First, elicited exocytosis demands Ca^{2+} influx through voltage-gated Ca^{2+} channels, and so there are two sources of cytosolic Ca^{2+}: that from influx and that from intracellular stores. The examination of spontaneous exocytosis allows us to examine the latter without activating the former, and hence circumvents the complication of two Ca^{2+} sources. Second, the study of spontaneous exocytosis has, since the time of Katz (1969), contributed valuable insights into the general process, most notably establishing the quantal or vesicular nature of exocytosis. Third, in neurons it is increasingly apparent that spontaneous exocytosis is not simply a byproduct of synaptic transmission but has a physiological role and is worth studying in its own right (see Glitsch, 2008) for the following reasons. In hippocampal CA1 pyramidal cells, spontaneous glutamate release maintains dendritic spines via AMPA receptor activation (McKinney et al., 1999). Moreover, spontaneous neurotransmitter release may regulate dendritic protein synthesis and thus influence expression of receptors on postsynaptic cells (Sutton and Carew, 2000). Furthermore, spontaneous neurotransmitter release can influence the processing of synaptic inputs in small interneurons and affect the interneuron's ability to fire action potentials (Carter and Regehr, 2002). Finally, short-term potentiation of miniature excitatory postsynaptic currents regulates excitability of postsynaptic supraoptic neurons in the hypothalamus (Kombian et al., 2000). Hence, in several neurons, spontaneous exocytosis has its own function.

Here, we find that preventing Ca^{2+} release from intracellular stores in the form of Ca^{2+} syntillas, in two different and independent ways, results in an increase in frequency and magnitude of spontaneous exocytotic events as measured by amperometry. The syntillas were monitored by using a unique high temporal and spatial resolution optical imaging system that permits monitoring of the entire cell and a "signal mass" analysis that measures the total amount of Ca^{2+} released per individual syntilla (see Materials and methods). Contrary to expectation, we conclude that Ca^{2+} syntillas inhibit spontaneous exocytosis of DCVs.

MATERIALS AND METHODS

Tight-seal whole cell recordings on chromaffin cells, freshly dissociated from adult male Swiss Webster mice as described previously (ZhuGe et al., 2006), were performed with an amplifier (EPC10; HEKA) on the same day as isolation. 6–8-wk-old mice were sacrificed by cervical dislocation in accordance with the Institutional Animal Care and Use Committee guidelines at the University of Massachusetts Medical School. Patch pipette solution was as follows (in mM): 0.05 K_5fluo-3 (Invitrogen), 135 KCl, 2 $MgCl_2$, 30 HEPES, 4 MgATP, and 0.3 Na-GTP, pH 7.3. The pipette solution buffered at 150 nM [Ca^{2+}] was the following (in mM): 0.025 K_5fura-2 (Invitrogen) or 0.05 K_5fluo-3, 0.25 EGTA, 0.175 $CaCl_2$, 135 KCl, 2 $MgCl_2$, 30 HEPES, 4 MgATP, and 0.3 Na-GTP, pH 7.3. The pipette solution buffered at 500 nM [Ca^{2+}] was the following (in mM): 0.025 K_5fura-2 (Invitrogen) or 0.05 K_5fluo-3, 0.1 EGTA, 0.1 $CaCl_2$, 135 KCl, 2 $MgCl_2$, 30 HEPES, 4 MgATP, and 0.3 Na-GTP, pH 7.3. EGTA, fura-2 or fluo-3, and $CaCl_2$ values were predicted with the free Ca^{2+} and Mg^{2+} program within IGOR Pro (WaveMetrics, Inc.) to achieve a free [Ca^{2+}] of 150 or 500 nM, and then adjusted based on measurements of global [Ca^{2+}]$_i$ with fura-2. The bath solution contained (in mM): 135 NaCl, 5 KCl, 10 HEPES, 10 glucose, 1 $MgCl_2$, and 2.2 $CaCl_2$, pH 7.2. Except when otherwise indicated, all reagents came from Sigma-Aldrich.

Fluorescence images using fluo-3 as a Ca^{2+} indicator were obtained using a custom-built wide-field digital imaging system described previously (ZhuGe et al., 2006). To assess the properties of individual Ca^{2+} syntillas quantitatively, the signal mass approach was used, as conceptualized by Sun et al. (1998) and developed for wide-field microscopy of Ca^{2+} sparks by ZhuGe et al. (2000). The purpose of this approach is to obtain a measure of the total amount of Ca^{2+} (as opposed to concentration of Ca^{2+}) released by a focal Ca^{2+} transient. Global [Ca^{2+}]$_i$ was measured by fluorescence with cell-impermeant fura-2 (25 µM) that was loaded into cells through the patch pipette and measured as described previously (Grynkiewicz et al., 1985; Becker and Fay, 1987; Drummond and Tuft, 1999).

Corrections for buffers in the calculations of signal mass, simulations for Fig. 6, and amperometric measurements are as follows. For the syntillas recorded in control and ryanodine experiments, where the only exogenous Ca^{2+} buffers were fluo-3 (50 µM) and ATP (4 mM), we corrected the signal mass value, as determined from the fluo-3 signal, for competition by endogenous Ca^{2+} buffer, as described previously (De Crescenzo et al., 2004; ZhuGe et al., 2006). In brief, a correction factor of 2.15 was calculated from the binding ratios at resting Ca^{2+} of the fluo-3, ATP, and the endogenous buffer. For the syntillas recorded in experiments where the resting [Ca^{2+}] was buffered to normal resting values with the addition of 250 µM EGTA and 175 µM Ca^{2+}, the fluo-3 signal mass was multiplied by 4.38 to account for the added competition by the EGTA. This number was determined empirically using computer simulations of the "typical" chromaffin syntilla (ZhuGe et al., 2006) with the addition of 250 µM EGTA, Kd = 180 nM, and koff = 0.45/s (Naraghi and Neher, 1997), and increasing the syntilla Ca^{2+} current magnitude until the fluo-3 signal mass equaled that in simulation without the EGTA. Note that this is much less than the factor of 17.46 that is predicted by equilibrium buffering, where the binding ratio of the EGTA is >600:1. The binding of Ca^{2+} by EGTA is too slow to significantly compete with fluo-3 over the few tens of milliseconds duration of a syntilla. Additionally, the simulations demonstrate that the effect of this amount of EGTA on the free [Ca^{2+}] spatiotemporal profile is negligible in the syntilla microdomain where high (>>1 µM) [Ca^{2+}] occurs.

Experimental protocols
Fluo-3 Ca^{2+} imaging and amperometry. After the patch is ruptured to provide the whole cell configuration, we waited at least

2 min for the fluo-3 to reach equilibrium in the cell. In a typical experiment, when the fluorescence was stable, we began to record two 4-s image sequences in a row (200 images separated by 20 ms, with an exposure time of 10 ms). Then, we started to record the amperometry for 4–6 min (two to three segments of 2 min each). After the amperometric recording, two more 4-s image sequences of fluo-3 fluorescence were recorded. These two image sequences and the ones recorded earlier were used to establish the syntilla frequency for that cell. These data show no difference between the frequency at the beginning and the frequency at the end of the experiments. So in a typical cell, both amperometry and fluo-3 fluorescence were recorded.

Ryanodine protocol. Ryanodine stock was first prepared in DMSO at 100 mM. Just before the experiments, ryanodine was dissolved in the physiological solution at 1/1,000 to reach the 100-µM concentration used. The cells were bathed in the 100-µM ryanodine solution in the dark for 30 min before recordings started.

In control, a caffeine pulse increased the basal $[Ca^{2+}]_i$ on average by 316 ± 91% ($n = 3$). $[Ca^{2+}]_i$ always returned to basal levels after the pulse. We found that after 30 min in ryanodine, the response to caffeine was minimal, inducing a mean increase of only 10 ± 2% above baseline ($n = 3$). Increasing the incubating time to 60 min in ryanodine in two cells did not further decrease the caffeine response (11 and 18% above baseline in response to caffeine).

Reserpine protocol. The cells were bathed in the 100-µM ryanodine solution (for control) or in 100 µM ryanodine plus 1 µM reserpine in the dark for 30 min before the experiments commenced (Mundorf et al., 2000; Gong et al., 2003). Preliminary experiments show that 1 µM reserpine alone compared with control (normal saline solution, in the absence of ryanodine) gave a significant decrease in the mean charge of amperometric spikes (0.21 ± 0.04 pC and $n = 6$ in control solution vs. 0.10 ± 0.01 pC and $n = 17$ in the presence of reserpine; P = 0.012). This 50% decrease is comparable to the reserpine effects (30% decrease) reported previously in adrenal chromaffin cells (Mundorf et al., 2000; Gong et al., 2003).

Thapsigargin (Tg) and caffeine protocols. See legend of Fig. 4 and Results.

Data analysis

Statistical analyses and plots were performed in OriginPro 8.0 (OriginLab). In all cases except for syntilla frequency and signal mass, data were first averaged per cell and are reported as mean ± SE of all cells. Data from syntilla frequency and signal mass are reported, as previously (ZhuGe et al., 2006), as mean ± SE of individual records and mean ± SE of individual syntillas, respectively. Statistical analysis of difference was made with a Student's t test (log-transformed for charge data) or a Mann-Whitney test (for syntilla frequencies), and the p-values are presented in the figure captions, as appropriate. A p-value <0.05 is significant except in multiple comparisons, where the Bonferroni-corrected p-values must be <0.02 (significance is indicated by an asterisk). n indicates the number of cells, except for syntilla frequency and signal mass, where n = number of records or syntillas, respectively.

Modeling the relationship between syntillas and exocytosis

We modeled the relationship between syntillas and the frequency of amperometric events in Fig. 6 B as a simple two-state system: vesicles that are able to release their catecholamines, and vesicles that are inhibited from releasing them by a process caused by a rise in $[Ca^{2+}]$ in a Ca^{2+} microdomain, which for purposes of fitting the data as seen in Fig. 6 B we define as a volume where free

$[Ca^{2+}]$ generated by a syntilla was >10 µM. The two-state model is represented as:

$$R \underset{\alpha}{\overset{\beta}{\underset{\rightarrow}{\leftarrow}}} I,$$

where α is the rate of inhibition due to syntillas and β is reverse rate to the releasable state. (We note that the syntilla microdomain could be set for any level of free $[Ca^{2+}]$, but 10 µM was chosen because it gave a slightly better fit to the data in Fig. 6 B and for several other reasons enumerated in Results. However, in Fig. 6 A we show the contour lines delimiting volumes corresponding to values of free $[Ca^{2+}]$ for 1, 3, 10, and 30 µM.) The number of releasable vesicles R, and therefore the observed frequency of amperometric events in this case, is:

$$f_{amp} \propto \left(\frac{\beta}{\beta + \alpha} \right). \quad (1)$$

We modeled α as proportional to the product of the syntilla frequency and the volume of the syntilla microdomain, which we call the syntilla index (SI):

$$SI = f_{syn} \cdot V_{syn}, \quad (2)$$

where f_{syn} is the syntilla frequency, and V_{syn} is the volume of the syntilla microdomain exceeding 10 µM of free $[Ca^{2+}]$. The units of SI are µm^3/s. Each of the four experimental conditions shown in Fig. 6 A (control, ryanodine, buffered control, and buffered Tg plus caffeine) has a corresponding SI value.

We can simplify by combining Eqs. 1 and 2 to obtain:

$$f_{amp} \propto \left(\frac{1}{1 + k * SI} \right), \quad (3)$$

where k*SI is equal to the ratio α/β.

The equation describing the frequency of amperometric events in vesicles/s at equilibrium is:

$$f_{amp} = F_0 * \left(\frac{1}{1 + k * SI} \right), \quad (4)$$

where F_0 is the frequency of events when syntillas are completely abolished (SI = 0). Assuming that the carbon fiber monitors ~10% of the cell surface (Haller et al., 1998; Grabner et al., 2005), whole cell amperometric frequencies were plotted against their corresponding SIs as seen in Fig. 6 B.

Determining syntilla microdomain volume

To determine the SI, it was first necessary to find the volume of the syntilla microdomain as defined above. To do this, we used the same approach as in ZhuGe et al. (2006), where we determined the spatiotemporal profile of free $[Ca^{2+}]$ using as input the I_{Ca} of the average chromaffin cell syntilla as derived from the first derivative of the average signal mass over time. We determined I_{Ca} from the average peak signal mass for each experimental condition in Fig. 6 (control, ryanodine, buffered control, and buffered Tg plus caffeine) using the time course found in ZhuGe et al. (2006). A computer simulation with the I_{Ca} for each condition as input was performed, and the resulting spatiotemporal profile of free $[Ca^{2+}]$ was established (Fig. 6 A). (The ordinate in Fig. 6 A represents one spatial dimension, with the other two being identical to the first. Together, they make up a hemisphere rather than a sphere because the RYR2s and hence the syntillas are in a

subplasmalemmal space where diffusion can only occur in a hemi-spherical volume.) The free $[Ca^{2+}]$ used to compute the volumes were 30, 10, 3, and 1 µM at their maximum spatial extent. For the SI, we used the 10 µM of free $[Ca^{2+}]$. The volumes were 0.02895, 0.00045, 0.0194, and 0.01435 µm^3 for control, ryanodine, buffered control, and buffered Tg plus caffeine, respectively. The corresponding syntilla frequencies were 0.81, 0.28, 0.78, and 0.42 s^{-1}, as shown in the bottom panel of Fig. 6 A. By Eq. 2, these gave SI values of 0.0235, 0.000126, 0.015, and 0.006 µm^3/s.

Amperometric measurements

Quantal release of catecholamine from single chromaffin cells was monitored electrochemically using carbon fiber electrodes with a tip diameter of 5.8 µm (ALA Scientific Instruments), as described previously (ZhuGe et al., 2006). Amperometric signals, i.e., oxidation currents, were monitored with a VA-10 amplifier (npi electronic GmbH), filtered at 0.5 kHz, digitized at 1 kHz with a Digidata 1200B acquisition system, and acquired with Patchmaster software from HEKA. Amperometric spikes were identified and analyzed using the Mini Analysis program (Synaptosoft, Inc.). Each event was visually inspected so that artifacts could be rejected from the analysis. The root mean square noise in acquired traces was typically <0.25 pA as determined by the Mini Analysis program. The detection threshold for an event was set to 2.5 times the baseline root mean square. Overlapping events were rare and were excluded from analysis. To minimize errors due to possible variation in exocytosis among cells from different animals, cells from each animal were divided into two groups: one as control, and the other treated with agents such as ryanodine. Stand-alone feet (SAFs) were separated from spikes based on criteria somewhat similar to Wang et al. (2006), where an index of event shape was used to evaluate the "rectangularity" of a putative SAF. In the present study, to qualify as an SAF, an event had to meet the criteria of an amplitude <2.5 pA and a ratio of full-width at half-height to event duration >0.25. Event durations for spikes and SAFs are defined as the duration between the time when the event signal exceeds and the time when it returns to the detection threshold amplitude as defined above.

RESULTS

For all experiments reported here, except for those of Fig. 3, freshly dissociated mouse adrenal chromaffin cells were studied in whole cell voltage clamp mode with the membrane potential held at −80 mV. Calcium indicator dyes were introduced through the patch pipette in the salt form, favoring its confinement to the cytosol and ensuring the same concentration from cell to cell; fluo-3 was used for detection of Ca^{2+} syntillas and fura-2 for measurement of global cytosolic $[Ca^{2+}]$. Amperometry was used to monitor individual exocytotic events.

Blocking RYRs

To examine the effect of Ca^{2+} stores on spontaneous exocytosis, we first used 100 µM ryanodine (see Materials and methods for protocol), which, as we have shown previously, blocks Ca^{2+} syntillas in mouse adrenal chromaffin cells (ZhuGe et al., 2006). Fig. 1 illustrates the fundamental findings of this first set of experiments. In Fig. 1 A, a cell is shown from a single image under control conditions (left) with a typical Ca^{2+} syntilla and

another cell bathed for 30 min in ryanodine (right) with syntillas decreased in frequency and amplitude (De Crescenzo et al., 2004; ZhuGe et al., 2006). This is due to block of RYRs, the Ca^{2+} channels embedded in
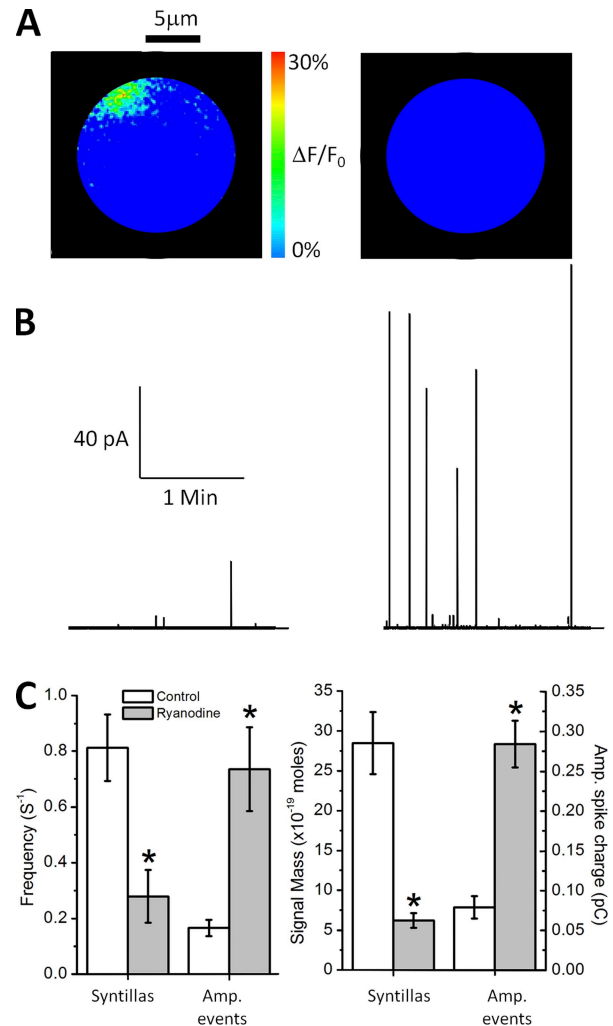

Figure 1. Effect of 100 µM ryanodine. (A) Changes in cytosolic $[Ca^{2+}]$ measured with the Ca^{2+}-indicator dye, fluo-3, and expressed on a pseudo-color scale as the change in fluorescence over the baseline fluorescence ($\Delta F/F_0$). Image threshold is 15% of $\Delta F/F_0$. Syntillas are larger and more frequent under normal conditions (left), and they are smaller and less frequent or completely blocked in the presence of ryanodine (right). (B) Representative amperometric trace from a cell in the absence (left) and presence (right) of ryanodine. In the presence of syntillas (left; control), amperometric events are smaller and less frequent. When syntillas are blocked or decreased (right; 100 µM ryanodine), amperometric events are larger and more frequent. (C; left) 100 µM ryanodine decreases syntilla frequency (left bar graph) from 0.81 ± 0.12 ($n = 4$) to 0.28 ± 0.09 s^{-1} ($n = 18$; P < 0.02). Conversely, ryanodine increases exocytotic frequency (right bar graph) from 0.16 ± 0.03 ($n = 12$) to 0.73 ± 0.15 s^{-1} ($n = 13$; P < 0.002). Error bars ± SEM. (Right) 100 µM ryanodine also decreases the mean signal mass of the individual syntilla from 28.5 ± 3.9 ($n = 13$) to $6.2 \pm 0.9 \times 10^{-20}$ moles ($n = 18$; P < 0.00001) and increases the mean charge per amperometric event from 0.08 ± 0.01 ($n = 12$) to 0.28 ± 0.03 pC ($n = 13$; P < 0.0003).

the ER membrane that are responsible for Ca^{2+} syntillas (De Crescenzo et al., 2004; ZhuGe et al., 2006) as well as Ca^{2+} sparks (Cheng and Lederer, 2008). In Fig. 1 B, typical amperometric traces are shown from a control (left) and ryanodine-treated (right) cell where individual events are more frequent and of larger amplitude. The Ca^{2+} syntillas decreased in frequency, whereas, quite surprisingly, the amperometric events increased in frequency upon treatment with ryanodine (Fig. 1 C, left). Moreover, the average magnitude of the individual Ca^{2+} syntilla as measured by its signal mass was decreased, whereas the mean charge per amperometric event increased (Fig. 1 C, right). (Simply put, the signal mass is a measure of the total amount of Ca^{2+} released per individual syntilla and hence it is given in units of moles of Ca^{2+}. See Materials and methods.)

The total charge per single spontaneous amperometric event (i.e., its magnitude) in the presence and absence of ryanodine is given in the distribution of Fig. 2 A, with the inset showing the difference between the two distributions; i.e., the additional events in the presence of ryanodine. These distributions count all events and show an increase in both their frequency and magnitude in the presence of ryanodine. When the events are separated into spikes and SAFs (Fig. 2, B and C), the frequency of the spikes, but not of the SAFs, is increased by ryanodine. Thus, the increase in frequency of spikes is not due to a shift from SAFs to spikes. SAFs are taken to represent partial vesicle emptying or "kiss and run" events, whereas spikes may represent either full fusion or "kiss and run" events (Wang et al., 2003; Gong et al., 2007). What accounts for the increase in the magnitude of the SAFs and spikes in the presence of ryanodine? In the case of the SAFs, which are approximated by a square wave, the amplitude alone is increased and not the duration. In the case of the spikes, the amplitude, rise time, and duration are all increased (Table I).

A change in global cytosolic Ca^{2+} concentration might be invoked to explain these results. However, global cytosolic Ca^{2+} concentration, as determined ratiometrically with fura-2, did not change in the presence of ryanodine (133.0 ± 28.4 nM [$n = 11$] vs. 140.0 ± 35.0 nM in control [$n = 5$]; P = 0.89). Furthermore, 100 µM ryanodine caused a decrease in the global calcium transient evoked by 20 mM caffeine (see ryanodine protocol in Materials and methods) as expected, showing that ryanodine was indeed blocking Ca^{2+} release via RYRs. Hence, there was no increase in global cytosolic $[Ca^{2+}]$ to explain the increase in amplitude and frequency of the spontaneous amperometric events. In sum, both the frequency and the magnitude of the amperometric spikes increased upon a decrease in the frequency and signal mass of the Ca^{2+} syntillas in the presence of ryanodine.

Blocking RYRs in the presence of reserpine

The ryanodine-induced increase in the frequency of exocytotic events is not readily explained by an inhibitory effect of syntillas on the vesicular monoamine transporter. Nevertheless, we examined the exocytotic events in the presence of reserpine to block the vesicular monoamine transporter with and without ryanodine. 1 µM reserpine was applied for at least 30 min (Mundorf et al., 2000; Gong et al., 2003) before recording, a standard
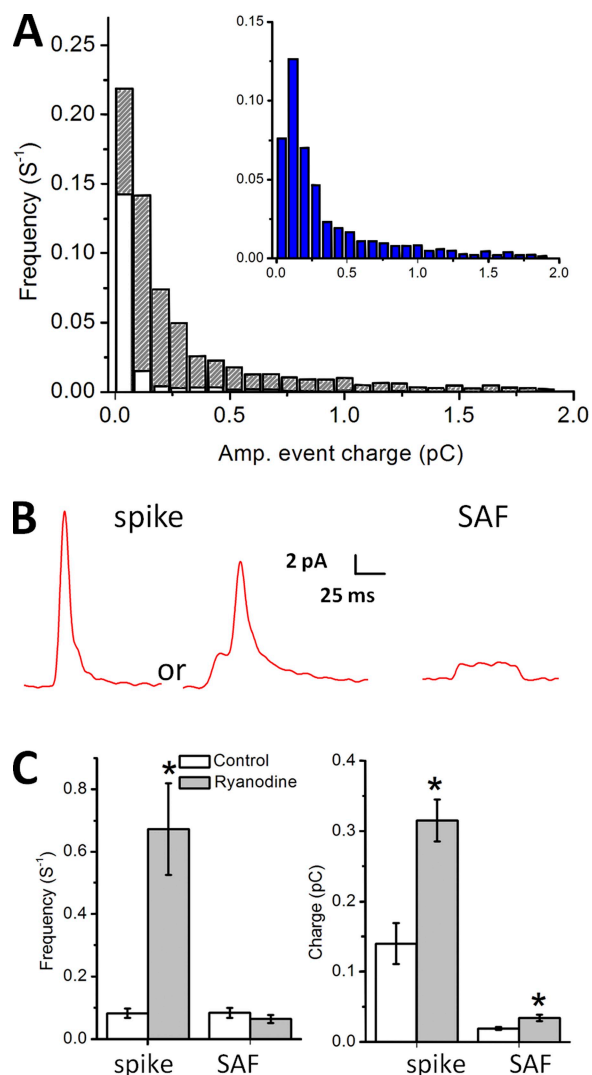

Figure 2. Population of DCVs blocked by ryanodine. (A) Frequency distribution of individual amperometric events according to charge (pC) in control (white; 918 events) and ryanodine-treated cells (stripes; 2,536 events). The difference between the two distributions is shown on an expanded x axis in the inset. (B) Examples of amperometric events recorded from mouse chromaffin cells. The first two traces show a spike, the second one with a pre-spike foot. The third one represents an SAF. (A includes all events, both SAFs and spikes. The criteria for classifying an event as an SAF are given in Materials and methods.) (C; left) The frequency of the spikes and the SAFs in control solution (0.08 ± 0.01 s^{-1} for both; $n = 12$). Spike frequency increases in the presence of ryanodine (0.67 ± 0.14 s^{-1}; P < 0.0008; $n = 13$). (Right) Ryanodine increases the mean charge of spikes (0.14 ± 0.03 to 0.31 ± 0.03 pC; P < 0.0003; $n = 12$ for control and $n = 13$ for treated cells) and SAFs (0.02 ± 0.00 to 0.04 ± 0.01 pC; P < 0.01; $n = 12$ for control and $n = 13$ for treated cells).

Parameter	Control mean ± SEM	100 µM ryanodine mean ± SEM	p-value
Spikes			
Amplitude (pA)	9.20 ± 2.3	15.90 ± 1.6	*0.026
Rise time[a] (ms)	6.78 ± 0.65	10.83 ± 0.95	*0.002
Half-width (ms)	11.79 ± 0.89	15.23 ± 1.5	0.068
τ[b] (ms)	11.45 ± 0.87	14.23 ± 1.38	0.099
Duration (ms)	62.99 ± 4.86	84.49 ± 7.56	*0.027
SAFs			
Amplitude (pA)	1.09 ± 0.03	1.84 ± 0.06	*0.000
Duration (ms)	32.68 ± 3.6	33.55 ± 4.3	0.877

p-values are from two sample Student's *t* tests.
[a]Rise time is 10–90%.
[b]τ is 67% decay.

protocol that was sufficient to exert the expected effects (see Materials and methods). However, reserpine did not block the effects of ryanodine on the frequency of amperometric events (0.12 ± 0.03 [$n = 17$] and 0.40 ± 0.13 s^{-1} [$n = 12$; P < 0.02] for reserpine and reserpine plus ryanodine, respectively) nor the mean charge increase (0.09 ± 0.01 [$n = 17$] and 0.26 ± 0.03 pC [$n = 12$; P < 0.00001] for reserpine and reserpine plus ryanodine, respectively).

Blocking RYRs in unpatched intact cells
In unpatched cells, we observed much the same spontaneous exocytotic activity as in whole cell recording. Furthermore, the same effects of ryanodine on amperometric events observed under conditions of whole cell recording are also seen in unpatched cells where the cytosol is not disturbed (Fig. 3 and Table II). Thus, the effect on spontaneous exocytosis extends beyond conditions of whole cell recording to intact cells.

Decreasing Ca^{2+} levels in ryanodine-sensitive internal stores
To examine the effect of Ca^{2+} stores in a way that did not depend on ryanodine blockade and that would provide another, independent line of evidence, we used Tg to deplete the Ca^{2+} stores. Tg, which blocks the sarco-ER Ca^{2+} ATPase (SERCA) pump that returns Ca^{2+} to the ER, by itself did not appear to cause substantial store depletion in the chromaffin cells because syntilla frequency did not decrease under this condition compared with its control (0.37 ± 0.11 vs. 0.46 ± 0.06 s^{-1}). This is to be expected when the stores have a minimal leak, as found, for example, in smooth muscle (ZhuGe et al., 1999). In that situation, not only is it necessary to prevent reuptake of Ca^{2+} into stores by blocking the SERCA pump, but caffeine also has to be used transiently to elicit release from the stores. Therefore, we treated the cells with Tg and then delivered a brief pulse of caffeine. Subsequently, after a 1-min pause to allow the cells to recover from the transient Ca^{2+} release, syntillas

Parameter	Control mean ± SEM	100 µM ryanodine mean ± SEM	p-value
Spikes			
Amplitude (pA)	6.9 ± 2.0	14.2 ± 2.1	*0.019
Rise time[a] (ms)	19.8 ± 1.3	12.1 ± 0.9	*0.00005
Half-width (ms)	21.2 ± 1.5	19.8 ± 1.2	0.47
τ[b] (ms)	23.2 ± 1.5	18.3 ± 0.9	*0.008
Duration (ms)	119.9 ± 11.0	89.2 ± 5.6	*0.018
SAFs			
Amplitude (pA)	1.7 ± 0.11	1.8 ± 0.08	0.53
Duration (ms)	68.5 ± 11.8	59.7 ± 8.79	0.56

p-values are from two sample Student's *t* tests.
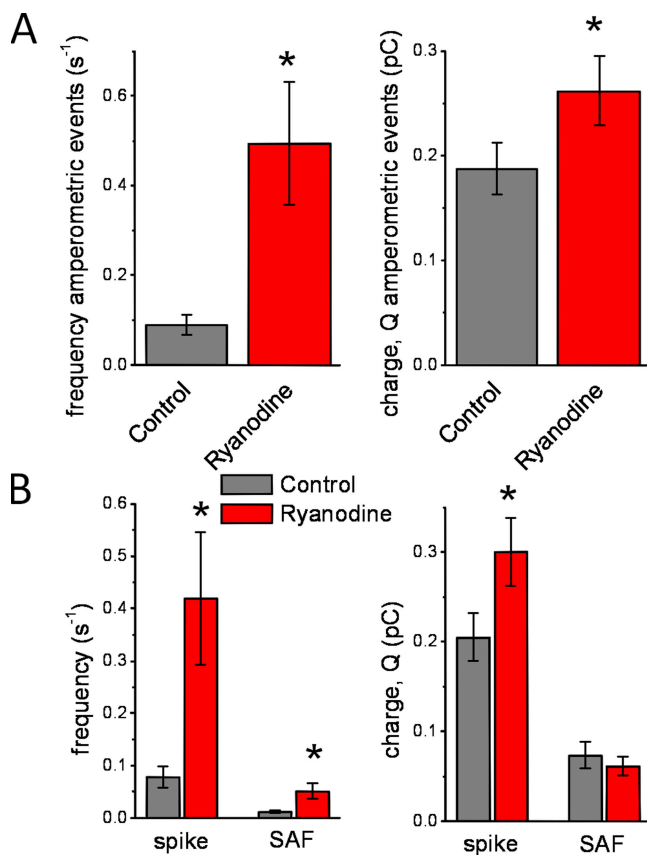[a]Rise time is 10–90%.
[b]τ is 67% decay.

Figure 3. Effect of 100 μM ryanodine in unpatched cells. In the results shown here, the same protocol was used as in Figs. 1 and 2, except that the cells were not patched and hence the cytosol was left undisturbed. (A) All amperometric events. (Left) The frequency of all events in control (0.09 ± 0.02 s^{-1}; $n = 28$) versus ryanodine (0.49 ± 0.14 s^{-1}; $n = 9$; P < 0.0002). (Right) The magnitude of all events for control (0.18 ± 0.2 pC; $n = 28$) versus ryanodine (0.26 ± 0.03 pC; $n = 9$; P < 0.02). (B) Amperometric events separated into spikes and SAFs. (Left) Control frequency of spikes (0.08 ± 0.02 s^{-1}; $n = 28$) and SAFs (0.01 ± 0.00 s^{-1}; $n = 28$) versus ryanodine for spikes (0.42 ± 0.13 s^{-1}; $n = 9$; P < 0.03) and for SAFs (0.05 ± 0.02 s^{-1}; $n = 9$; P < 0.02). (Right) The magnitude of spikes (0.20 ± 0.03 pC; $n = 28$) and SAFs (0.07 ± 0.01 pC; $n = 21$) in control versus ryanodine for spikes (0.30 ± 0.04 pC; $n = 9$; P < 0.02) and for SAFs (0.06 ± 0.01 pC; $n = 9$; P = 0.6).

and exocytosis were monitored over 4–6 min (Fig. 4 A). Neither Tg alone nor caffeine alone had an effect on syntillas or amperometric events as compared with the data under control conditions as shown in Figs. 1 and 2. Tg plus caffeine decreased the frequency of syntillas compared with Tg alone or caffeine alone (Fig. 4 B). In the second case, that is, when caffeine was puffed in the absence of Tg, syntillas were recorded after 1 min. Only with the Tg plus caffeine protocol did we find a corresponding increase in the frequency of both spikes and SAFs (Fig. 4 C). The charge of amperometric events was not significantly altered (Fig. 4 D). However, when we measured global [Ca^{2+}] in each condition, we found that Tg plus caffeine caused a rise in mean global cytosolic [Ca^{2+}] to ∼500 nM (Fig. 4 E). This rise in global

[Ca^{2+}] was a confounding condition because it has been reported that elevation of global calcium can facilitate the spontaneous release of granules in cultured bovine adrenal chromaffin cells (Augustine and Neher, 1992) over a range of [Ca^{2+}]$_i$ levels above 200 nM and saturating at 10 μM.

To distinguish the possible effect of the elevated global [Ca^{2+}] from that of syntillas, we experimentally separated them in two ways. First, we buffered the internal solution to 500 nM to study only the effect of a higher global [Ca^{2+}]. Second, we buffered the internal solution to 150 nM, the approximate resting level (see below), and applied Tg plus caffeine to study the effect of lower Ca^{2+} syntilla frequency alone without a global increase.

To do this, we first buffered the internal solution with Ca^{2+} and EGTA to mimic the increased global Ca^{2+} levels in the Tg plus caffeine experiments and monitored both syntillas and amperometric events. The results are shown in Fig. 4, in the rightmost columns in green. We detected no difference in the frequency of syntillas when global Ca^{2+} was elevated to 500 nM (Fig. 4 B). Nor did we find an increase in the frequency or charge of amperometric events when the resting global Ca^{2+} was raised from 135 to 500 nM (Fig. 4, C and D). This was to be expected, however, because significant facilitation of granule release was not achieved until [Ca^{2+}]$_i$ reached levels near 1 μM in Augustine and Neher (1992).

Next, we buffered the internal cytosolic [Ca^{2+}] to 150 nM with EGTA introduced through the patch pipette (Fig. 5). With this buffering, the global [Ca^{2+}] in control cells versus Tg alone or Tg plus caffeine–treated cells was not different (P > 0.025), as determined with ratiometric fura-2 measurements (control: 106 ± 9 nM [$n = 4$] vs. Tg alone: 127 ± 30 [$n = 6$; P = 0.53l]; and control vs. Tg plus caffeine: 176.4 ± 38 nM [$n = 5$; P = 0.14]). Moreover, these levels were well below the 500-nM concentration, which itself was without detectable effect on the amperometric events (see previous paragraph.) Upon Tg plus caffeine treatment in the buffered condition, we again saw a decrease in the syntilla frequency and an increase in frequency and magnitude of amperometric events as we did when RYRs were blocked with ryanodine (Fig. 5 A). The distribution of the total charge per amperometric event in control and treated cells is shown in Fig. 5 B. The distribution of the amperometric events suppressed by release of Ca^{2+} from stores is shown in the inset of Fig. 5 B. As with the experiments using ryanodine, there was an increase in spike frequency without change in SAF frequency (Fig. 5 C). There was an increase in the mean magnitude of all the amperometric events, which was evident when the spikes and SAFs were grouped together (Fig. 5 A), although this was not as marked as that observed with ryanodine (Fig. 1 C). However, there was no increase in the rise time of spikes nor in SAF amplitude (Table III), in contrast to the experiments with ryanodine. (Hence,
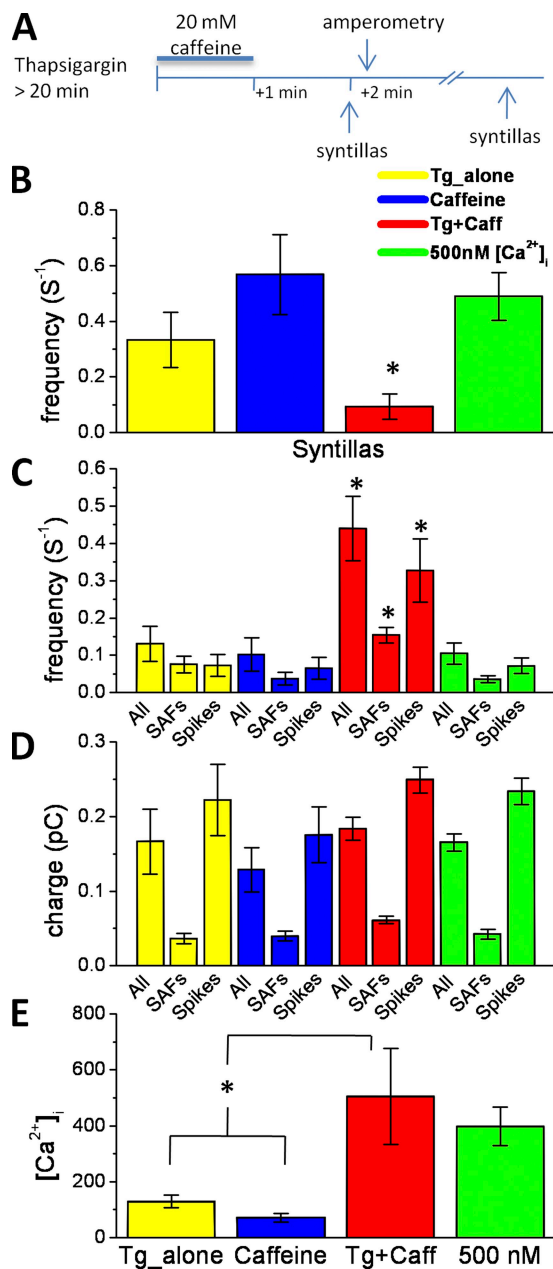
Figure 4. Effect of 2 μM Tg plus 20 mM caffeine and buffering free $[Ca^{2+}]_i$ at 500 nM with EGTA and $CaCl_2$. (A) Diagram representing the protocol to decrease the stores with Tg and caffeine. (B) Tg and caffeine decrease syntilla frequency to 0.09 ± 0.04 s^{-1} ($n = 8$) compared with Tg alone (0.33 ± 0.09 s^{-1}; $n = 15$; $P < 0.04$), caffeine alone (0.57 ± 0.14 s^{-1}; $n = 12$; $P < 0.01$), and with the free $[Ca^{2+}]_i$ buffered at 500 nM (0.49 ± 0.08 s^{-1}; $n = 23$; $P < 0.001$). (C) Tg and caffeine increase the frequency of all amperometric events to 0.44 ± 0.09 s^{-1} ($n = 8$), SAFs to 0.15 ± 0.02 s^{-1} ($n = 8$), and spikes to 0.33 ± 0.09 s^{-1} ($n = 8$) when compared with Tg alone (0.13 ± 0.05 s^{-1}; $n = 9$; $P < 0.01$) for all events: 0.08 ± 0.02 s^{-1} ($n = 7$; $P < 0.02$) for SAFs, 0.07 ± 0.03 s^{-1} ($n = 9$; $P < 0.02$) for spikes, and caffeine alone (0.10 ± 0.04 s^{-1}; $n = 10$; $P < 0.01$) for all events; 0.04 ± 0.02 s^{-1} ($n = 10$; $P < 0.001$) for SAFs, 0.07 ± 0.03 s^{-1} ($n = 10$; $P < 0.02$) for spikes, and when the free $[Ca^{2+}]_i$ is buffered at 500 nM (0.10 ± 0.03 s^{-1}; $n = 10$; $P < 0.01$) for all events: 0.04 ± 0.01 s^{-1} ($n = 9$; $P < 0.001$) for SAFs and 0.07 ± 0.02 s^{-1} ($n = 10$; $P < 0.02$) for spikes. (D) Tg and caffeine do not alter the quantal charge of amperometric events, compared with Tg alone, caffeine alone, or when the free $[Ca^{2+}]_i$ is buffered at 500 nM. (E) Tg and caffeine increase global $[Ca^{2+}]_i$ to 505.3 ± 172 nM ($n = 5$) compared with typical basal global $[Ca^{2+}]_i$ in Tg alone (130.0 ± 23 nM; $n = 7$; $P < 0.03$) and caffeine alone (71.4 ± 16 nM; $n = 7$; $P < 0.02$). When free $[Ca^{2+}]_i$ is buffered at 500 nM, the mean basal global $[Ca^{2+}]_i$ (397.8 ± 69 nM; $n = 6$) is not significantly different compared with Tg and caffeine ($P = 0.59$). Error bars, ±SEM.

the change in amplitude of amperometric events seen in Fig. 5 A appears to simply be a consequence of an increase in spike frequency without a change in SAF frequency (Fig. 5 C).) Finally, the amplitude of the syntillas in these experiments did not change (Fig. 5 A), again in contrast to the experiments with ryanodine (Fig. 1 C). The mean signal mass of the syntillas as given in Fig. 5 A has been corrected for the EGTA buffering as outlined in Materials and methods. With this correction, the signal mass does not differ from the signal mass in unbuffered solution (Fig. 1 C), whereas the frequency of syntillas has decreased. This is reminiscent of the finding with Ca^{2+} sparks in smooth muscle, where a partial depletion of the ER results in a decrease in spark frequency without a change in amplitude. The reason appears to be that a small reduction of $[Ca^{2+}]$ in the ER regulates spark frequency even when that reduction is not sufficient to result in a substantially smaller driving force on the Ca^{2+} (ZhuGe et al., 1999). The results from the experiments using buffered internal solutions show that the global $[Ca^{2+}]$ in the range of 150 to 500 nM has no detectable effect on spontaneous exocytosis.

The results with Tg and caffeine, collectively with those of ryanodine above, argue against an effect mediated by the level of the $[Ca^{2+}]$ in the ER, for example, an effect on the store-operated channels, because in one case the stores are depleted while in the other they are not. The results with Tg and caffeine also indicate that the effect on release is an acute effect. The effect occurs within minutes after the application of caffeine, a time too short for vesicle synthesis or recycling (Wakade et al., 1988; von Grafenstein and Knight, 1992).

Relationship between exocytotic events and syntillas

The data from the experiments reported here were used to construct a plot of the relationship between Ca^{2+} syntillas and the frequency of spontaneous amperometric events (Fig. 6 B). We devised an SI, which is the product of the syntilla rate and the volume of the syntilla microdomain, as defined in Materials and methods and shown in Fig. 6 A. We show four spatiotemporal contour lines delimiting volumes of four $[Ca^{2+}]$'s within the syntilla microdomain (from 1 to 30 μM) (Fig. 6 A). We do not provide a contour line for lower $[Ca^{2+}]$ because buffering the global $[Ca^{2+}]$ to 500 nM was without effect on spontaneous amperometric events. Similarly, a target that can only be affected by a $[Ca^{2+}]$ an order of

TABLE III
Spike and SAF parameters: control versus Tg plus Caff buffered

Parameter	Control mean ± SEM	Tg plus Caff mean ± SEM	p-value
Spikes			
Amplitude (pA)	8.56 ± 1.9	9.71 ± 2.6	0.726
Rise time[a] (ms)	9.41 ± 0.93	8.63 ± 0.88	0.552
Half-width (ms)	12.72 ± 0.84	12.1 ± 0.89	0.615
Tau[b] (ms)	13.22 ± 1.2	12.0 ± 1.2	0.462
Duration (ms)	69.79 ± 4.0	65.00 ± 4.3	0.424
SAFs			
Amplitude (pA)	1.15 ± 0.06	1.31 ± 0.13	0.306
Duration (ms)	38.81 ± 4.0	33.10 ± 5.5	0.414

p-values are from two sample Student's *t* tests.
[a]Rise time is 10–90%.
[b]τ is 67% decay.

magnitude higher than 30 μM has no precedent so far as we know. The syntilla rate for each experimental condition is summarized directly underneath the contour lines in Fig. 6 A. The relationship between Ca^{2+} syntillas and amperometric event frequency (Fig. 6 B) was fitted by assuming that the vesicles reached a state where they could be exocytosed, and the action of a syntilla, directly or indirectly, resulted in the inhibition of that state.

DISCUSSION

The central finding of this study is that decreasing the frequency of Ca^{2+} syntillas leads to an increase in the frequency and magnitude of spontaneous exocytosis. We therefore propose, as the simplest explanation, that syntillas exert an inhibitory influence over spontaneous exocytosis. The result cannot easily be explained by hitherto unknown effects of the agents used to produce the decrease in syntilla frequency because we used two quite different sets of agents in separate experiments, whose effects have been studied in considerable detail over decades. Our results also rule out two explanations for the findings. First, the increase in magnitude of the amperometric events observed upon blocking syntillas does not seem to be due to a change in vesicle filling because it is not affected by reserpine (see Results). Second, a trivial explanation for the increase in frequency of amperometric events might be that an increase in magnitude improves detection, thus making it appear that the frequency has risen. For this to be the case, there would need to be smaller undetected events in the control condition. But when we lowered the threshold for inclusion in the data from 0.5 to 0.2 pA, we found only 21 more events in addition to the 918 in Fig. 2 A, which would increase the frequency by ~2.3%. This is far from sufficient to account for the 450% increase observed in the presence of ryanodine (Fig. 2 C). Moreover, in the experiments with Tg plus caffeine, the frequency of spikes increases but the charge apparently

does not. Finally, the same effects on amperometric events are found when ryanodine is applied to intact, unpatched cells.

A second Ca^{2+} microdomain
The increase in exocytotic frequency and magnitude upon blocking syntillas is quite unexpected, given the usual role attributed to Ca^{2+} in the exocytotic process. Nevertheless, at least one precedent exists for such a result, and that is the effect of the analogue of syntillas, Ca^{2+} sparks, in smooth muscle. In that case, sparks, by activating Ca^{2+}-sensitive, large conductance K^+ channels within the spark microdomain, elicit current that hyperpolarizes the membrane, thus turning off voltage-activated Ca^{2+} channels and causing relaxation. This effect is precisely the opposite of what might be expected of cytosolic Ca^{2+} in muscle (Nelson et al., 1995). This mechanism of relaxation depends on the action of Ca^{2+} in a distinct microdomain, calculated to be within a radius of 150–300 nm from the Ca^{2+} release site (ZhuGe et al., 2002). We suggest that in adrenal chromaffin cells, the syntillas act in a different microdomain from that where the final exocytotic step occurs. This conclusion is borne out by a previous study, as well as the present one, in which Ca^{2+} syntillas, despite their ability to raise $[Ca^{2+}]$ to super-micromolar levels within their microdomain, do not elicit exocytosis (ZhuGe et al., 2006). One microdomain might be termed the exocytotic domain where the voltage-gated Ca^{2+} channels responsible for elicited exocytosis are found and the final exocytotic steps are triggered by Ca^{2+}, and the other, the syntilla microdomain, where RYR2s are present and Ca^{2+} has an inhibitory effect on spontaneous exocytosis.

Physiological role of spontaneous exocytosis and its regulation by syntillas
Is the spontaneous exocytosis examined here of physiological significance? And is the regulation exerted by the syntillas on catecholamine release of quantitative
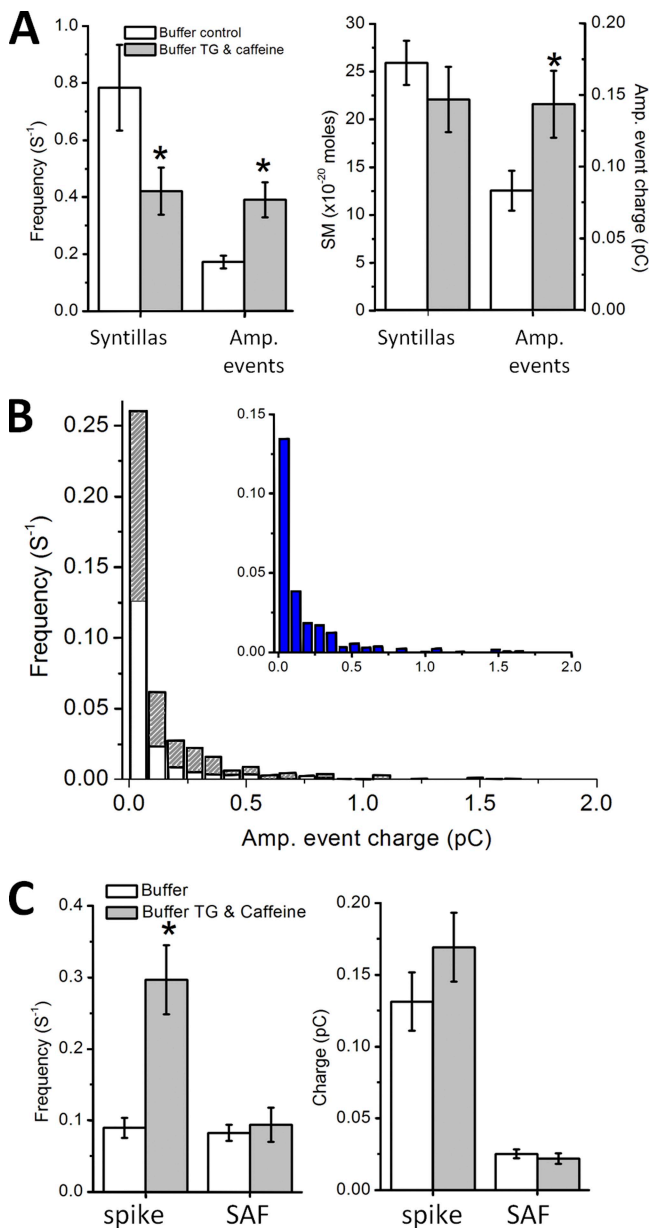
Figure 5. Effect of 2 µM Tg with caffeine. Chromaffin cells were treated with 2 µM of the SERCA inhibitor Tg for 20 min or longer and briefly exposed (1 min) to 20 mM caffeine by picospritzer to reduce internal Ca^{2+} stores. (A; left) When Ca^{2+} stores are reduced and cytosolic Ca^{2+} is buffered with EGTA as described in Materials and methods, the mean frequency of syntillas is reduced from 0.78 ± 0.15 ($n = 15$) to 0.42 ± 0.01 s^{-1} ($n = 23$; $P < 0.03$), and the amperometric event frequency is increased from 0.17 ± 0.02 ($n = 20$) to 0.39 ± 0.06 s^{-1} ($n = 10$; $P < 0.0003$). (Right) When the stores are reduced, there is no detectable change in the mean syntilla signal mass (25.9 ± 2.3 [$n = 47$] and 22.1 ± 3.4 [$n = 36$], control and treated, respectively), but the mean charge of amperometric events increases (0.083 ± 0.014 [$n = 20$] and 0.143 ± 0.023 pC [$n = 10$; $P < 0.026$]). A and B include both spikes and SAFs. (B) Frequency distribution of individual amperometric events according to charge (pC) in control (white; 731 events) and when stores are reduced by Tg and caffeine treatment (stripes; 908 events). The difference between the two distributions is shown on an expanded x axis in the inset in blue. (C; left) The frequency in control solution with buffer (0.09 ± 0.01 s^{-1} for spikes and 0.08 ± 0.01 s^{-1}

importance? We can gain some insight into these questions by comparing our results with recent work from the Smith laboratory (Fulop et al., 2005; Doreian et al., 2008, 2009) on physiological levels of stimulation of mouse chromaffin cells. These investigators call attention to two different physiological types of stimulation: a low frequency (0.5 Hz) and a high frequency (15 Hz) corresponding, respectively, to resting sympathetic tone and "stress-associated" sympathetic activation (Brandt et al., 1976; Kidokoro and Ritchie, 1980).

Fulop et al. (2005) found a rate of ~0.93 amperometric events per second per amperometric site per cell for both stimulus paradigms, the difference in the two conditions being primarily the magnitude of the individual events. In our study, the rate was 0.16 ± 0.03 s^{-1} in control conditions and 0.73 ± 0.15 s^{-1} in the presence of ryanodine when virtually all syntillas were blocked. Thus, the rate when syntillas are suppressed is 66% of that at physiological levels of stimulation. (If the plot in Fig. 6 is extrapolated to zero syntilla rate, the rate of amperometric events achieved by a physiological stimulation level [0.93 s^{-1}] and the rate achieved by syntilla suppression [0.78 s^{-1}] are of the same magnitude.)

Physiologically, in terms of relevance to the whole organism, it is of some interest to examine the rate of catecholamine release, i.e., moles s^{-1} of catecholamines. At the lower physiological stimulation rate of 0.5 Hz, Fulop et al. (2005) measured 200 pC of catecholamines for a mean rate of 1.73 aM s^{-1} of catecholamine per amperometric site per cell. (At their higher rate of 15 Hz, Fulop et al. [2005] found that the amount of catecholamine released per second [M s^{-1}] approximately doubled.) We measured 0.06 aM s^{-1} of catecholamine per amperometric site per cell under control conditions and 1.06 aM s^{-1} of catecholamine in the presence of ryanodine, which almost completely suppressed the syntillas. Several points deserve mention. First, the effect of suppressing syntillas on the rate of spontaneous catecholamine release is not trivial, amounting to more than a 10-fold increase. In fact, it is greater than that of increasing the stimulation from 0.5 to 15 Hz, which results in an approximate twofold increase in the rate of catecholamine release. Second, the rate of catecholamine release when syntillas are almost completely suppressed (1.06 aM s^{-1}) is 62% of that at 0.5 Hz (1.73 aM s^{-1}). That is, the two values are of the same order of magnitude, the intriguing implications of which have not eluded our notice. From these considerations, we

for SAFs) is the same as in control solution without buffer as given in Fig. 2 C. After treatment with Tg and caffeine, the spike frequency increases to 0.30 ± 0.05 s^{-1} ($P < 0.00002$; $n = 10$). (Right) The mean charge of spikes (0.13 ± 0.02 vs. 0.17 ± 0.02 pC) or SAFs (0.02 ± 0.00 pC for control and treatment) in control and after Tg plus caffeine treatment.

suggest that syntillas may well be a potent physiological regulator of catecholamine release.

The parameters of individual exocytotic events at the two levels of physiological stimulation have also been measured (supplemental data in Doreian et al., 2008, 2009) and can be compared with spontaneous events in the present study. First, the mean amperometric amplitude and magnitude with basal stimulation at 0.5 Hz (4.0 ± 0.43 pA and 0.08 ± 0.01 pC) are the same as spontaneous release (5.4 ± 1.3 pA and 0.08 ± 0.01 pC). Moreover, when spontaneous syntillas are suppressed with ryanodine, the mean amplitude and charge (14.5 pA and 0.28 pC) are the same as reported for stimulation at 15 Hz (16.3 pA and 0.31 pC). In sum, when the amplitude and magnitude of individual amperometric events are considered, suppression of syntillas with ryanodine yields the same increase as stimulation at 15 Hz. Therefore, Ca^{2+} store modulation of spontaneous release may involve the mechanisms invoked by the Smith group to describe differences in 0.5- versus 15-Hz stimulation, i.e, a change in mode of release from kiss and run to full fusion. This points to the possible relevance of the mechanisms affecting spontaneous release for understanding elicited release at physiological levels of stimulation.

Dual effect of syntillas on spontaneous exocytosis

The two effects of suppressing syntillas on spontaneous exocytosis, increasing the frequency and increasing the magnitude, might be linked or independent. If the increase in frequency and the increase in charge are indeed distinct effects, how might this happen? We propose that some DCVs exposed to the syntilla microdomain are simply removed temporarily from the releasable pool, and so the frequency of spontaneous exocytosis goes down. Other vesicles exposed to Ca^{2+} in the syntilla microdomain would have their pore machinery modified, resulting in less catecholamine release. This effect is reminiscent of the findings of Alés et al. (1999), where greater Ca^{2+} influx caused a shift away from full fusion and toward kiss and run events. The larger Ca^{2+} influx in that study, resulting from extracellular Ca^{2+} concentrations as high as 90 mM, might have impinged on the Ca^{2+} syntilla microdomain and thus mimicked the effects of syntillas.
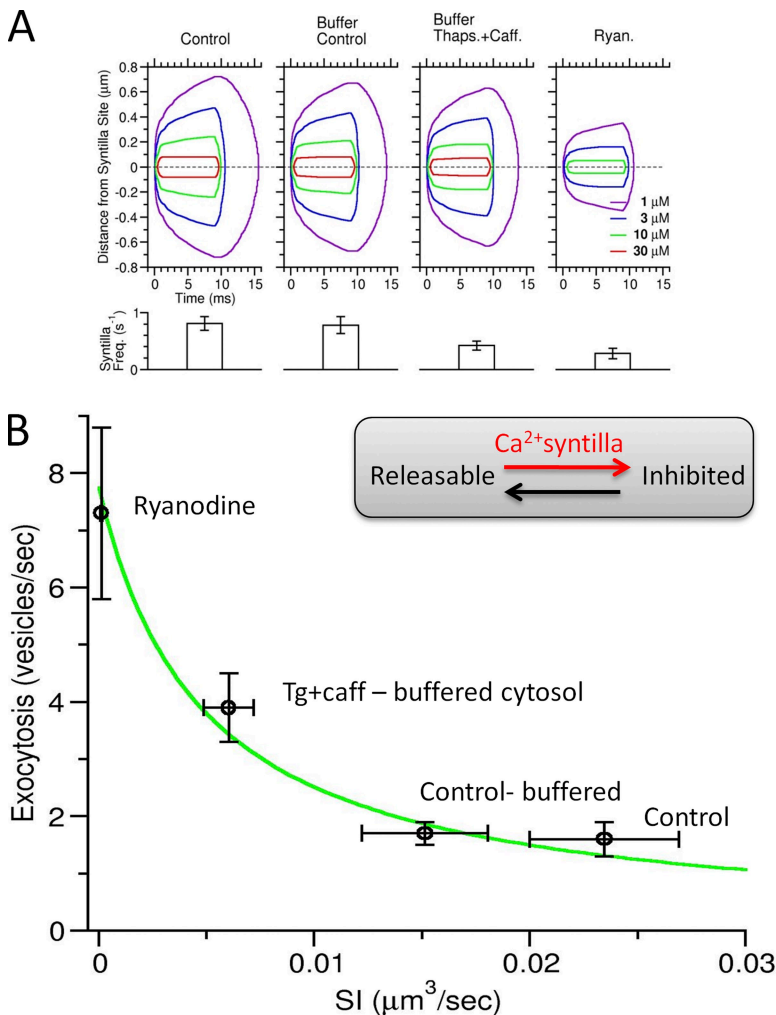

Figure 6. Relationship between Ca^{2+} released into the syntilla microdomain and exocytotic events. (A; top) Spatiotemporal profiles of the Ca^{2+} syntilla arising from RYR2s near the plasma membrane for each experimental condition. Concentric curves represent different $[Ca^{2+}]$'s within the syntilla microdomain. Note that the ordinate presents one of the spatial axes; the other two are the same as the one shown and together constitute a hemisphere (see Materials and methods). (Bottom) Syntilla frequency for each of the four experimental conditions listed above the top panel. (B) Relationship of the SI for the entire cell versus frequency of exocytotic events from the entire cell surface. The plot shows that the frequency of amperometric events declines to a baseline level as the SI increases. The relationship drawn here is based on a 10-µM syntilla microdomain (A, green line). The equation of the curve to which the data are fit:

$$f_{amp} = F_0 * \left(\frac{1}{1 + k * SI} \right) \qquad (4)$$

is based on a two-state model as described in Materials and methods, where DCVs are either in an inhibited or releasable state. A least-squares fit of Eq. 4 to the data points in B was performed, resulting in $F_0 = 7.75$ and $k = 104.10$. The correlation coefficient (R^2) of the fit is 0.993.

A second hypothesis is that block of Ca^{2+} syntillas causes greater recruitment of a population of larger DCVs. Such a population has been observed in mouse chromaffin cells both morphologically and physiologically (Grabner et al., 2005). In this case, the observed changes in the parameters of the amperometric spikes are consistent with a larger DCV being exocytosed through a pore of the same size as that of the smaller DCVs, which is opening at the same rate. On one hand, such a shift from a population of smaller DCVs to larger ones is attractive because it explains both the changes in frequency and the magnitude of amperometric events by a single mechanism. On the other hand, the effects of blocking syntillas on the magnitude and frequency of amperometric events seem separable, so that they may indeed be different effects.

Molecular components of regulation of spontaneous exocytosis by syntillas

The molecular components of the inhibitory effect of Ca^{2+} syntillas on spontaneous exocytosis are only partially known at this point. Clearly, RYRs—more specifically, RYR2s, the "cardiac" type, mediate the effect. The evidence for this comes from a previous study in which we detected high levels of RYR2 by RT-PCR, but only low levels of RYR3 and virtually no trace of RYR1 (ZhuGe et al., 2006). By immunocytochemistry, there was no trace of RYR1, and RYR3 was found only in an isolated clump in the cell center. In contrast, RYR2 was found in a subplasmalemmal distribution throughout the cell (ZhuGe et al., 2006), which seems to be consistent with the localization of syntillas by imaging. In addition, the ability of Tg to affect the syntillas indicates that the SERCA pump is also involved in replenishing the Ca^{2+} that appears in the form of syntillas.

Ultimately, the syntillas must affect either the vesicles or the plasmalemmal sites of spontaneous fusion. One simple mechanism that could account for the decrease in frequency is that the DCVs carry with them a Ca^{2+} sensor that detects the syntilla and inhibits or limits the DCVs' ability to complex with the exocytotic machinery. It is tempting to postulate that this sensor is synaptotagmin. In the absence of the T-SNARE complex at the plasma membrane, synaptotagmin will undergo a cis interaction with the vesicle membrane in the presence of elevated $[Ca^{2+}]$ (Hui et al., 2005; Stein et al., 2007). Such an interaction renders the synaptotagmin incapable of complexing with the T-SNARE complex at the plasma membrane. The source of Ca^{2+} to disable the synaptotagmin might be provided by the Ca^{2+} syntilla before the DCV reaches the plasma membrane. If the effect of Ca^{2+} syntillas were targeted to only a population of large vesicles, this hypothesis could explain both the increase in frequency and magnitude. Alternatively, the Ca^{2+} sensor might have more than one effect; for example, the vesicles that are not completely inhibited might be rendered less competent to undergo complete emptying, resulting in smaller magnitude of the fusion events.

Another attractive hypothesis involves the subplasmalemmal filamentous actin (F-actin) mesh. It is well documented in chromaffin cells that dissolution of the dense actin cortex is necessary to sustain recruitment of DCVs to the membrane during stimulation (Nakata and Hirokawa, 1992; Vitale et al., 1995; Tchakarov et al., 1998; Giner et al., 2007). Therefore, syntillas could play a role in maintaining the actin mesh under spontaneous conditions. If the actin network breaks down in the absence of syntillas, this could explain the increase in frequency of amperometric events observed in the presence of ryanodine. But it could also explain the increase in quantal size of events. Doreian et al. (2008, 2009) have shown that disruption of F-actin favors the full fusion mode of exocytosis over kiss and run. That is, one role of the intact dense F-actin mesh in mouse chromaffin cells is to stabilize the fusion pore during exocytosis and keep it from expanding to full fusion. If syntillas help stabilize the F-actin mesh, their absence would actually have two effects: (1) more DCVs recruited to the membrane (actin mesh as the barrier); and (2) DCVs at the membrane would primarily undergo full fusion exocytosis. In support of this idea, it is interesting that Doreian et al. (2009) find a mean amplitude and charge of 4.0 ± 0.43 pA and 0.08 ± 0.01 pC for events that undergo kiss and run exocytosis that is similar to the mean amplitude and charge of amperometric events we record under spontaneous control conditions (5.4 ± 1. 3 pA and 0.08 ± 0.01pC, respectively). Moreover, the same study finds a mean amplitude and charge of 16.3 pA and 0.31 pC for full fusion events, when the actin network is broken down during high frequency stimulation, which compares well with our mean amplitude and charge of events recorded in ryanodine (14.5 pA and 0.28 pC).

In conclusion, it is clear that the Ca^{2+} syntilla adds to the diversity of tasks for which Ca^{2+} can be used in the process of exocytosis.

REFERENCES

Alés, E., L. Tabares, J.M. Poyato, V. Valero, M. Lindau, and G. Alvarez de Toledo. 1999. High calcium concentrations shift the mode of exocytosis to the kiss-and-run mechanism. *Nat. Cell Biol.* 1:40–44. doi:10.1038/9012

Augustine, G.J., and E. Neher. 1992. Calcium requirements for secretion in bovine chromaffin cells. *J. Physiol.* 450:247–271.

Becker, P.L., and F.S. Fay. 1987. Photobleaching of fura-2 and its effect on determination of calcium concentrations. *Am. J. Physiol.* 253:C613–C618.

Brandt, B.L., S. Hagiwara, Y. Kidokoro, and S. Miyazaki. 1976. Action potentials in the rat chromaffin cell and effects of acetylcholine. *J. Physiol.* 263:417–439.

Carter, A.G., and W.G. Regehr. 2002. Quantal events shape cerebellar interneuron firing. *Nat. Neurosci.* 5:1309–1318. doi:10.1038/nn970

Cheng, H., and W.J. Lederer. 2008. Calcium sparks. *Physiol. Rev.* 88:1491–1545. doi:10.1152/physrev.00030.2007

Collin, T., A. Marty, and I. Llano. 2005. Presynaptic calcium stores and synaptic transmission. *Curr. Opin. Neurobiol.* 15:275–281. doi:10.1016/j.conb.2005.05.003

Csernoch, L. 2007. Sparks and embers of skeletal muscle: the exciting events of contractile activation. *Pflugers Arch.* 454:869–878. doi:10.1007/s00424-007-0244-0

De Crescenzo, V., R. ZhuGe, C. Velázquez-Marrero, L.M. Lifshitz, E. Custer, J. Carmichael, F.A. Lai, R.A. Tuft, K.E. Fogarty, J.R. Lemos, and J.V. Walsh Jr. 2004. Ca2+ syntillas, miniature Ca2+ release events in terminals of hypothalamic neurons, are increased in frequency by depolarization in the absence of Ca2+ influx. *J. Neurosci.* 24:1226–1235. doi:10.1523/JNEUROSCI.4286-03.2004

Doreian, B.W., T.G. Fulop, and C.B. Smith. 2008. Myosin II activation and actin reorganization regulate the mode of quantal exocytosis in mouse adrenal chromaffin cells. *J. Neurosci.* 28:4470–4478. doi:10.1523/JNEUROSCI.0008-08.2008

Doreian, B.W., T.G. Fulop, R.L. Meklemburg, and C.B. Smith. 2009. Cortical F-actin, the exocytic mode and neuropeptide release in mouse chromaffin cells is regulated by MARCKS and myosin II. *Mol. Biol. Cell.* 20:3142–3154.

Drummond, R.M., and R.A. Tuft. 1999. Release of Ca2+ from the sarcoplasmic reticulum increases mitochondrial [Ca2+] in rat pulmonary artery smooth muscle cells. *J. Physiol.* 516:139–147. doi:10.1111/j.1469-7793.1999.139aa.x

Fulop, T., S. Radabaugh, and C. Smith. 2005. Activity-dependent differential transmitter release in mouse adrenal chromaffin cells. *J. Neurosci.* 25:7324–7332. doi:10.1523/JNEUROSCI.2042-05.2005

García, A.G., A.M. García-De-Diego, L. Gandía, R. Borges, and J. García-Sancho. 2006. Calcium signaling and exocytosis in adrenal chromaffin cells. *Physiol. Rev.* 86:1093–1131. doi:10.1152/physrev.00039.2005

Giner, D., I. López, J. Villanueva, V. Torres, S. Viniegra, and L.M. Gutiérrez. 2007. Vesicle movements are governed by the size and dynamics of F-actin cytoskeletal structures in bovine chromaffin cells. *Neuroscience.* 146:659–669. doi:10.1016/j.neuroscience.2007.02.039

Glitsch, M.D. 2008. Spontaneous neurotransmitter release and Ca2+—how spontaneous is spontaneous neurotransmitter release? *Cell Calcium.* 43:9–15. doi:10.1016/j.ceca.2007.02.008

Gong, L.W., I. Hafez, G. Alvarez de Toledo, and M. Lindau. 2003. Secretory vesicles membrane area is regulated in tandem with quantal size in chromaffin cells. *J. Neurosci.* 23:7917–7921.

Gong, L.W., G.A. de Toledo, and M. Lindau. 2007. Exocytotic catecholamine release is not associated with cation flux through channels in the vesicle membrane but Na+ influx through the fusion pore. *Nat. Cell Biol.* 9:915–922. doi:10.1038/ncb1617

Grabner, C.P., S.D. Price, A. Lysakowski, and A.P. Fox. 2005. Mouse chromaffin cells have two populations of dense core vesicles. *J. Neurophysiol.* 94:2093–2104. doi:10.1152/jn.00316.2005

Grynkiewicz, G., M. Poenie, and R.Y. Tsien. 1985. A new generation of Ca2+ indicators with greatly improved fluorescence properties. *J. Biol. Chem.* 260:3440–3450.

Haller, M., C. Heinemann, R.H. Chow R. Heidelberger, and E. Neher. 1998. Comparison of secretory responses as measured by membrane capacitance and by amperometry. *Biophys. J.* 74:2100–2113.

Hui, E., J. Bai, P. Wang, M. Sugimori, R.R. Llinas, and E.R. Chapman. 2005. Three distinct kinetic groupings of the synaptotagmin family: candidate sensors for rapid and delayed exocytosis. *Proc. Natl. Acad. Sci. USA.* 102:5210–5214. doi:10.1073/pnas.0500941102

Katz, B. 1969. The Release of Neural Transmitter Substances. Liverpool University Press, Liverpool. 60 pp.

Kidokoro, Y., and A.K. Ritchie. 1980. Chromaffin cell action potentials and their possible role in adrenaline secretion from rat adrenal medulla. *J. Physiol.* 307:199–216.

Kombian, S.B., M. Hirasawa, D. Mouginot, X. Chen, and Q.J. Pittman. 2000. Short-term potentiation of miniature excitatory synaptic currents causes excitation of supraoptic neurons. *J. Neurophysiol.* 83:2542–2553.

McKinney, R.A., M. Capogna, R. Dürr, B.H. Gähwiler, and S.M. Thompson. 1999. Miniature synaptic events maintain dendritic spines via AMPA receptor activation. *Nat. Neurosci.* 2:44–49. doi:10.1038/4548

Mundorf, M.L., K.P. Troyer, S.E. Hochstetler, J.A. Near, and R.M. Wightman. 2000. Vesicular Ca(2+) participates in the catalysis of exocytosis. *J. Biol. Chem.* 275:9136–9142. doi:10.1074/jbc.275.13.9136

Nakata, T., and N. Hirokawa. 1992. Organization of cortical cytoskeleton of cultured chromaffin cells and involvement in secretion as revealed by quick-freeze, deep-etching, and double-label immunoelectron microscopy. *J. Neurosci.* 12:2186–2197.

Naraghi, M., and E. Neher. 1997. Linearized buffered Ca2+ diffusion in microdomains and its implications for calculation of [Ca2+] at the mouth of a calcium channel. *J. Neurosci.* 17:6961–6973.

Neher, E., and T. Sakaba. 2008. Multiple roles of calcium ions in the regulation of neurotransmitter release. *Neuron.* 59:861–872. doi:10.1016/j.neuron.2008.08.019

Nelson, M.T., H. Cheng, M. Rubart, L.F. Santana, A.D. Bonev, H.J. Knot, and W.J. Lederer. 1995. Relaxation of arterial smooth muscle by calcium sparks. *Science.* 270:633–637. doi:10.1126/science.270.5236.633

Stein, A., A. Radhakrishnan, D. Riedel, D. Fasshauer, and R. Jahn. 2007. Synaptotagmin activates membrane fusion through a Ca2+-dependent trans interaction with phospholipids. *Nat. Struct. Mol. Biol.* 14:904–911. doi:10.1038/nsmb1305

Sun, X.P., N. Callamaras, J.S. Marchant, and I. Parker. 1998. A continuum of InsP3-mediated elementary Ca2+ signalling events in Xenopus oocytes. *J. Physiol.* 509:67–80. doi:10.1111/j.1469-7793.1998.067bo.x

Sutton, M.A., and T.J. Carew. 2000. Parallel molecular pathways mediate expression of distinct forms of intermediate-term facilitation at tail sensory-motor synapses in Aplysia. *Neuron.* 26:219–231. doi:10.1016/S0896-6273(00)81152-6

Tchakarov, L.E., L. Zhang, S.D. Rosé, R. Tang, and J.M. Trifaró. 1998. Light and electron microscopic study of changes in the organization of the cortical actin cytoskeleton during chromaffin cell secretion. *J. Histochem. Cytochem.* 46:193–203.

Vitale, M.L., E.P. Seward, and J.M. Trifaró. 1995. Chromaffin cell cortical actin network dynamics control the size of the release-ready vesicle pool and the initial rate of exocytosis. *Neuron.* 14:353–363. doi:10.1016/0896-6273(95)90291-0

von Grafenstein, H., and D.E. Knight. 1992. Membrane recapture and early triggered secretion from the newly formed endocytotic compartment in bovine chromaffin cells. *J. Physiol.* 453:15–31.

Wakade, A.R., T.D. Wakade, and R.K. Malhotra. 1988. Restoration of catecholamine content of previously depleted adrenal medulla in vitro: importance of synthesis in maintaining the catecholamine stores. *J. Neurochem.* 51:820–829. doi:10.1111/j.1471-4159.1988.tb01817.x

Wang, C.T., J.C. Lu, J. Bai, P.Y. Chang, T.F. Martin, E.R. Chapman, and M.B. Jackson. 2003. Different domains of synaptotagmin control the choice between kiss-and-run and full fusion. *Nature.* 424:943–947. doi:10.1038/nature01857

Wang, C.T., J. Bai, P.Y. Chang, E.R. Chapman, and M.B. Jackson. 2006. Synaptotagmin-Ca2+ triggers two sequential steps in regulated

exocytosis in rat PC12 cells: fusion pore opening and fusion pore dilation. *J. Physiol.* 570:295–307.

ZhuGe, R., S.M. Sims, R.A. Tuft, K.E. Fogarty, and J.V. Walsh Jr. 1998. Ca2+ sparks activate K+ and Cl- channels, resulting in spontaneous transient currents in guinea-pig tracheal myocytes. *J. Physiol.* 513:711–718. doi:10.1111/j.1469-7793.1998.711ba.x

ZhuGe, R., R.A. Tuft, K.E. Fogarty, K. Bellve, F.S. Fay, and J.V. Walsh Jr. 1999. The influence of sarcoplasmic reticulum Ca^{2+} concentration on Ca^{2+} sparks and spontaneous transient outward currents in single smooth muscle cells. *J. Gen. Physiol.* 113:215–228. doi:10.1085/jgp.113.2.215

ZhuGe, R., K.E. Fogarty, R.A. Tuft, L.M. Lifshitz, K. Sayar, and J.V. Walsh Jr. 2000. Dynamics of signaling between Ca^{2+} sparks and Ca^{2+}-activated K^+ channels studied with a novel image-based method for direct intracellular measurement of ryanodine receptor Ca^{2+} current. *J. Gen. Physiol.* 116:845–864. doi:10.1085/jgp.116.6.845

ZhuGe, R., K.E. Fogarty, R.A. Tuft, and J.V. Walsh Jr. 2002. Spontaneous transient outward currents arise from microdomains where BK channels are exposed to a mean Ca^{2+} concentration on the order of 10 μM during a Ca^{2+} spark. *J. Gen. Physiol.* 120:15–27. doi:10.1085/jgp.20028571

ZhuGe, R., V. DeCrescenzo, V. Sorrentino, F.A. Lai, R.A. Tuft, L.M. Lifshitz, J.R. Lemos, C. Smith, K.E. Fogarty, and J.V. Walsh Jr. 2006. Syntillas release Ca2+ at a site different from the microdomain where exocytosis occurs in mouse chromaffin cells. *Biophys. J.* 90:2027–2037. doi:10.1529/biophysj.105.071654